RESEARCH ARTICLE

Different Mode of Afferents Determines the Frequency Range of High Frequency Activities in the Human Brain: Direct Electrocorticographic Comparison between Peripheral Nerve and Direct Cortical Stimulation

Katsuya Kobayashi[1], Riki Matsumoto[2]*, Masao Matsuhashi[3], Kiyohide Usami[1], Akihiro Shimotake[1], Takeharu Kunieda[4], Takayuki Kikuchi[4], Nobuhiro Mikuni[5], Susumu Miyamoto[4], Hidenao Fukuyama[3], Ryosuke Takahashi[1], Akio Ikeda[2]*

1 Department of Neurology, Kyoto University Graduate School of Medicine, Kyoto, Japan, 2 Department of Epilepsy, Movement Disorders and Physiology, Kyoto University Graduate School of Medicine, Kyoto, Japan, 3 Human Brain Research Center, Kyoto University Graduate School of Medicine, Kyoto, Japan, 4 Department of Neurosurgery, Kyoto University Graduate School of Medicine, Kyoto, Japan, 5 Department of Neurosurgery, Sapporo Medical University School of Medicine, Sapporo, Hokkaido, Japan

* matsumot@kuhp.kyoto-u.ac.jp (RM); akio@kuhp.kyoto-u.ac.jp (AI)

Abstract

Physiological high frequency activities (HFA) are related to various brain functions. Factors, however, regulating its frequency have not been well elucidated in humans. To validate the hypothesis that different propagation modes (thalamo-cortical vs. cortico-coritcal projections), or different terminal layers (layer IV vs. layer II/III) affect its frequency, we, in the primary somatosensory cortex (SI), compared HFAs induced by median nerve stimulation with those induced by electrical stimulation of the cortex connecting to SI. We employed 6 patients who underwent chronic subdural electrode implantation for presurgical evaluation. We evaluated the HFA power values in reference to the baseline overriding N20 (earliest cortical response) and N80 (late response) of somatosensory evoked potentials ($HFA_{SEP(N20)}$ and $HFA_{SEP(N80)}$) and compared those overriding N1 and N2 (first and second responses) of cortico-cortical evoked potentials ($HFA_{CCEP(N1)}$ and $HFA_{CCEP(N2)}$). $HFA_{SEP(N20)}$ showed the power peak in the frequency above 200 Hz, while $HFA_{CCEP(N1)}$ had its power peak in the frequency below 200 Hz. Different propagation modes and/or different terminal layers seemed to determine HFA frequency. Since $HFA_{CCEP(N1)}$ and HFA induced during various brain functions share a similar broadband profile of the power spectrum, cortico-coritcal horizontal propagation seems to represent common mode of neural transmission for processing these functions.

Introduction

In the last decade, advancement in technology has made it possible to analyze ultra slow or high frequency activities (HFAs), or high frequency oscillations (HFOs) in the human brain. Neuronal functional networks show the broadband oscillatory activities ranging from 0.01 Hz to 600 Hz or above. In particular, neuronal activities above the conventional gamma range are reported to be specific to the each content of neuronal functional activities in both physiological and pathological neuronal processes [1–3].

Physiologically, gamma oscillations, in particular, those above 60 Hz (60–200 Hz) are closely associated with brain functions such as motor [1,4–6], language [7–8], attention [9], auditory [10–11], and visual [12] functions. Neuronal activities of the conventional 'narrowband' gamma (below 60–80 Hz) have been reported to originate from neuronal synchronization mainly by inhibitory interneuron networks [13–15], and those of 'broadband' high gamma (80–200 Hz) have been reported to reflect increase of the multiunit activities or local field potentials [16–18].

Much before the discovery of high gamma activities related with various brain functions, faster activity around 600 Hz was discovered and intensively investigated in somatosensory function by recording somatosensory evoked potentials (SEPs) [19–29]. This activity was different from the aforementioned activities in that it is an evoked activity that overrides the early cortical component (N20) of median nerve SEP. The generator of HFOs or HFAs of SEP (HFA$_{SEP}$) has been proposed at various locations: the terminal segments of the thalamocortical fibers [30], the primary somatosensory cortex (SI) close to the generator of SEP N20 [31], GABAergic inhibitory fast-spiking interneurons at SI [26], and subcortical neurons [32]. Among them, the main generator has been proposed at or around SI from findings obtained by direct electrocorticographic recording. HFA$_{SEP}$ seems to play an important role in sensory information processing, and their impairment is reported in patients with multiple sclerosis, migraine and epilepsy [33–36].

The pathological high frequency oscillations (HFOs) or HFAs have been recently explored in the field of epilepsy, and nowadays are regarded as one of the possible biomarkers of epileptogenicity [37–39]. Pathological HFAs are generally divided into ripples between 100 and 200 Hz and fast ripples more than 250 Hz [2]. The generator of pathological HFAs, especially fast ripples, is presumably single or recurrent population spikes that reflect summated hypersynchronized discharges of principal cells [40–41].

Besides intrinsic physiological or pathological HFAs, external stimulation can generate cortical HFAs. In addition to the peripheral nerve stimulation that generates HFA$_{SEP}$, direct electrical cortical stimulation can produce HFOs. Electrical stimulation of the piriform cortex produced oscillatory gamma responses (50–60 Hz) mainly at the layer Ia (superficial layer) in normal rats [42]. Moreover a recent study has shown that pathological HFAs could reliably be produced by electrical microstimulation of the hippocampus in the tetanus toxin-induced epileptic rats and normal rats [43].

Although the mechanisms how HFAs are generated have been studied both *in vivo and vitro* in animals [44–45], factors regulating the frequency of physiological (60–200 Hz for cognitive HFA, ~600 Hz for HFA$_{SEP}$) and pathological (epileptic: 80–500 Hz) HFAs have not been well elucidated in humans. We focused on the SI cortex to investigate factors regulating physiological HFAs since HFA$_{SEP}$ (~600 Hz) has been extensively studied in humans. We hypothesized that different modes of propagation, vertical (thalamo-cortical) vs. horizontal (cortico-cortical) projections, or different terminal layers, i.e., layer IV vs. layer II/III affect the frequency of physiological HFAs. We compared HFAs in SI triggered by median nerve stimulation with those elicited by single pulse electrical cortical stimulation (SPES). Cortico-cortical

evoked potentials (CCEPs) have been widely used to evaluate the cortical evoked response to SPES [46]. CCEPs are recorded from the adjacent and remote cortices by averaging electrocorticograms (ECoGs) time-locked to the single pulse stimuli. CCEPs usually consist of an early negative component (N1) and a late negative component (N2). This method has been used for investigating cortico-cortical connections involved in functional brain systems [46–54] or seizure networks [55–56]. In the present study, by applying SPES to the cortex connecting to SI, we focused on the HFAs overriding CCEP N1 and N2 components in the SI cortex and compared their feature with HFA$_{SEP}$. In the present study, we adopted the terminology of "HFAs" for all the high frequency activities although "HFOs" have been used in the previous studies of the high frequency activities overriding SEPs. This is because we do not only focus on the 'narrowband' high frequency activities showing discrete oscillatory activities but also the 'broadband' activities.

Materials and Methods

Patients

Six patients (2 female), 4 with medically intractable partial epilepsy and 2 with brain tumor were studied (Table 1). All underwent chronic subdural electrode implantation covering the peri-rolandic area for the presurgical evaluation. In all but patient 5, the epileptic foci were away from the peri-rolandic area. In patient 5, although the lesion (brain tumor) was in the peri-rolandic area, the hand SI was located outside the lesion. Because of the ill-defined ictal onset in the scalp EEG and normal MRI findings, patient 1 underwent electrode implantation twice: the first implantation in the bilateral hemispheres to lateralize the seizure onset, and the second one in the right hemisphere to localize the epileptic focus. Therefore we measured SEPs and CCEPs in 7 hemispheres from 6 patient, i.e., 2 hemispheres from patient 1—patient 1L and patient 1R. Neurological examination was normal except patient 5 who showed slight paresis in the right lower extremity. The implanted electrodes were made of platinum with a recording diameter of 2.3 mm and a center-to-center interelectrode distance of 1 cm (Ad-Tech, Rachine, WI, USA) or with a recording diameter of 3 mm and a center-to-center interelectrode distance of 1 cm (Unique Medical Co., Ltd., Tokyo, Japan). As a part of the clinical presurgical evaluation, high frequency (50 Hz) electrical stimulation was performed for functional cortical mapping. Cortical mapping of the peri-rolandic area was performed in patients 3–6. To define the exact location of each electrode on the brain, subdural electrodes were co-registered to

Table 1. Patient profile.

Patient	1		2	3	4	5	6
Age, gender	23F		24M	29M	34M	40M	28F
Handedness	R		R	L	L	R	R
Epilepsy	FLE		FLE	TLE	Parieto-temporal Lobe Epilepsy	Peri-rolandic Epilepsy	PLE
Etiology	FCD type IA		FCD type IB	FCD type IA and HS	Posttraumatic injury and ischemic change (parietal) and HS and dysplastic change (temporal)	Oligoastrocytoma	DNT
Neurological Examination	Normal		Normal	Normal	Normal	Slight right lower extremity weakness	Normal
Recording hemisphere	L	R	L	L	R	L	R

FLE = frontal lobe epilepsy, TLE = temporal lobe epilepsy, PLE = parietal lobe epilepsy, FCD = focal cortical dysplasia, HS = hippocampal sclerosis, DNT = dysembryoplastic neuroepithelial tumor

doi:10.1371/journal.pone.0130461.t001

three dimensional volume-rendered MRIs, which were reconstructed from MPRAGE taken while electrodes were in place. The location of each electrode was identified on the 2D-MRI by using its signal void due to the property of the platinum alloy. The methodological details have been described elsewhere [46,57]. The central sulcus (CS) and its relationship to the electrodes were also identified by anatomical landmarks on the 3D-MRI.

The present study was approved by the Ethics Committee of Kyoto University Graduate School of Medicine (No. 443). Written informed consent was obtained from all patients.

Data Acquisition of SEPs

Electrocorticograms (ECoGs) were recorded with a bandpass filter of 0.016–600 Hz and a sampling rate of 2,000 Hz in all patients (EEG-1100, Nihon Kohden, Tokyo, Japan) and analyzed off-line using Matlab software (Matlab version 7.12.0; the MathWorks Inc., MA). Cortical recordings from subdural electrodes were referenced to a scalp electrode placed on the skin over the mastoid process contralateral (patient 1R and 2–6) or ipsilateral (patient 1L) to the side of electrode implantation.

The median nerve contralateral to the side of electrode implantation was stimulated at the wrist (a square wave pulse of 0.3 ms duration at 0.3 Hz) (Electrical Stimulator SEN-7203, Nihon Kohden, Tokyo, Japan). The stimulus intensity was adjusted to 20% above the motor threshold. In all the patiens, SEPs were recorded before tapering the antiepileptic drugs in the first week of chronic electrode implantation. During recording, the patients were lying on the bed and requested not to perform any specific task under awake condition. At least 2 trials of 150 sweeps were averaged to confirm the reproducibility of responses. SEPs were obtained by off-line averaging ECoGs time-locked to the stimulus onset with a time window of 1,000 ms (from 300 ms before to 700 ms after the stimulus onset). The baseline was set for the first 200 ms: from 300 ms to 100 ms before the stimulus onset.

Data Acquisition of CCEPs

The methodological details of CCEPs have been described elsewhere [46,49]. In brief, electrical stimulation was applied in a bipolar manner to a pair of adjacently placed subdural electrodes by a constant-current stimulator (MEE-1232, Nihon Kohden, Tokyo, Japan). The single pulse electrical stimuli (a square wave pulse of 0.3 ms duration) were delivered in alternating polarity at a fixed frequency of 1 Hz. In the previous CCEP study, the CCEP consisted of an early (N1) and a late (N2) negative potentials, and the latencies of N1 and N2 usually ranged 10–50 ms and 100–200 ms, respectively. The stimulus intensity was set at 6–12 mA after confirming the absence of afterdischarges (ADs) and excessive artifacts that obscured the CCEP waveform.

ECoGs were recorded with a bandpass filter of 0.08–600 Hz. The sampling rate and reference electrode setting were the same as those for SEPs. During the recording of CCEPs, the patients were lying on the bed and requested not to perform any specific task under awake condition. In all the patients, CCEPs were recorded in the second week after returning the dosage of antiepileptic drugs. At least 2 trials of 30–50 responses each were averaged to confirm the reproducibility of responses. CCEPs were obtained off-line by averaging ECoGs time-locked to the stimulus onset. The time window (1,000 ms) and baseline (200 ms) was set as the same as those of SEPs. The method has been reported elsewhere in detail [46,58].

Definition of the Primary Sensory Cortex (SI) and Selection of CCEPs in the hand SI

In this study, we aimed at comparing HFAs overriding SEPs and CCEPs in the hand SI. The hand SI electrode was identified according to the largest cortical SEP component, N20. We

confirmed the location of the hand SI electrodes on the postcentral gyrus anatomically by the 3D-MRI in all patients. The epileptic focus was away from the hand SI in all patients. No patients showed interictal epileptic spikes at the hand SI electrode.

We usually perform SPES to most of the implanted electrodes in order to investigate the cortico-cortical connections involved in seizure propagation and brain functions for clinical purposes. For this particular study, we selected the stimulus sites (electrode pairs) that produced large outstanding CCEP waveforms at the hand SI electrode in each patient. The subsequent time frequency analysis was performed for the ECoG data for each CCEP stimulus site. In other words, when the robust CCEP waveform was recorded in the hand SI from more than 1 stimulus site (e.g., 2 stimulus sites) in 1 patient, the time frequency analysis was performed for each stimulus site separately.

Time Frequency Analysis

A time-frequency representation was built for each epoch of raw ECoG data recorded during SEP and CCEP recording by using the short-time Fourier Transform (STFT). The epoch duration was the same as that used for SEP and CCEP analyses, i.e., from 300 ms before to 700 ms after the stimulus onset. The analysis frequency range was 0–600 Hz. The Fourier Transform was performed on 25 data-point window (12.5 ms; frequency resolution 80 Hz) at each time-step. The step of the sliding window was set at 5 ms; in other words, 1 time bin was with width of 5 ms centered at 2.5 ms. A Hanning window was imposed on each window to attenuate edge effects.

With the current amplifier (EEG-1100, Nihon Kohden, Tokyo, Japan), the stimulus artifact lasts up to 3–4 ms from the stimulus onset. A preliminary CCEP latency analysis revealed that N1 peaked between 7–27 ms at the SI electrode. In order to differentiate the stimulus artifact from the N1 potential for the STFT anlaysis, we selected the short window size of 25 points (12.5 ms) and sacrificed the frequency resolution to 80 Hz. When we analyze the high frequency activities, it is important to distinguish the evoked response that is time-locked and phase-locked to the stimulation from the induced response that is time-locked, but not phase-locked. Induced (non-phase-locked) responses are analyzed by subtracting event-related potential from the raw ECoG signal in each individual trial to minimize the contribution of evoked (phase-locked) responses [59]. In this study, our aim was to analyze neuronal activities induced by external stimulation upon individual trial basis. Therefore, in contrast to the most of the previous somatosensory evoked HFA studies, we adopted induced HFA responses for SEPs in the same condition as those of CCEPs.

After the STFT, we averaged the power spectrum across all the epochs. The logarithmic power spectrum (base 10) was computed for the given frequency range and window. The baseline for computation was set to the same as that for averaging SEP and CCEP: from 300 ms to 100 ms before the stimulus onset. We refer to the stimulus-locked induced HFA for SEP data as "HFA_{SEP}" and that for CCEP data as "HFA_{CCEP}" herein for clarity. For HFA_{CCEP} analysis, we focused on the induced HFA overriding the early N1 potential ($HFA_{CCEP(N1)}$) and the following N2 potential ($HFA_{CCEP(N2)}$). Since the N1 is regarded as the first volley reaching the target cortex [49,51,60], HFA overriding N20 ($HFA_{SEP(N20)}$) was analyzed as an N1 counterpart. HFA overriding N80 ($HFA_{SEP(N80)}$), a late cortical component subsequent to the early cortical component, was also analyzed since the peak latency was closest to that of N2. As for HFAs on the early potentials ($HFA_{SEP(N20)}$, $HFA_{CCEP(N1)}$), the power changes were calculated for 1 time bin that included the peak of SEP N20 or CCEP N1. We carefully selected a bin after 15 ms for evaluating $HFA_{CCEP(N1)}$ and $HFA_{SEP(N20)}$ so that the 25 data-point (12.5 ms) window did not overlap with the stimulus artifact in all patients. CCEP N1 peaked, however, before 12.5 ms in 2 CCEP responses, and we selected the bin at 15 ms instead in order to avoid stimulus artifact

on these rare occasions. We selected 4 bins (mean of 20 ms bin at and around the peak) for calculating the power spectra of CCEP N2 and SEP N80. We confirmed the validity of the usage of the bin after 15 ms for evaluating $HFA_{CCEP(N1)}$ and $HFA_{SEP(N20)}$, namely, that the 25 data-point (12.5 ms) window did not overlap with the stimulus artifact, by performing an additional stimulus artifact analysis using the dead pig brain (see S1 Text and S1 Fig).

Since most of the aforementioned induced HFA activities were within 200 ms from the stimulus onset, we displayed the STFT results across the whole time points and frequencies in 3 dimensions (time, frequency, and power value) in a time window of 220 ms (from 20 ms before to 200 ms after the stimulus onset) in figures (Figs 1B, 2B, 3A and 3B).

In order to compare the power trend across the frequency bands among $HFA_{SEP(N20)}$, $HFA_{SEP(N80)}$, $HFA_{CCEP(N1)}$, and $HFA_{CCEP(N2)}$, we also drew additional figures plotting the change of the logarithmic power spectra across the frequency bands at the timing of N1 and N2 of CCEP and N20 and N80 of SEP. In each patient, we analyzed the power values for frequency bands centered at 80, 160, 240, 320, 400, 480, and 560 Hz for the 4 groups ($HFA_{SEP(N20)}$, $HFA_{SEP(N80)}$, $HFA_{CCEP(N1)}$, $HFA_{CCEP(N2)}$). After the plot was made for each patient (see Fig 3G, 3H, 3I and 3J), all the power values from 7 hemispheres in 6 patients (N = 7 for $HFA_{SEP(N20)}$ and $HFA_{SEP(N80)}$, N = 16 for $HFA_{CCEP(N1)}$ and $HFA_{CCEP(N2)}$) were plotted in the same figure (see Fig 4).
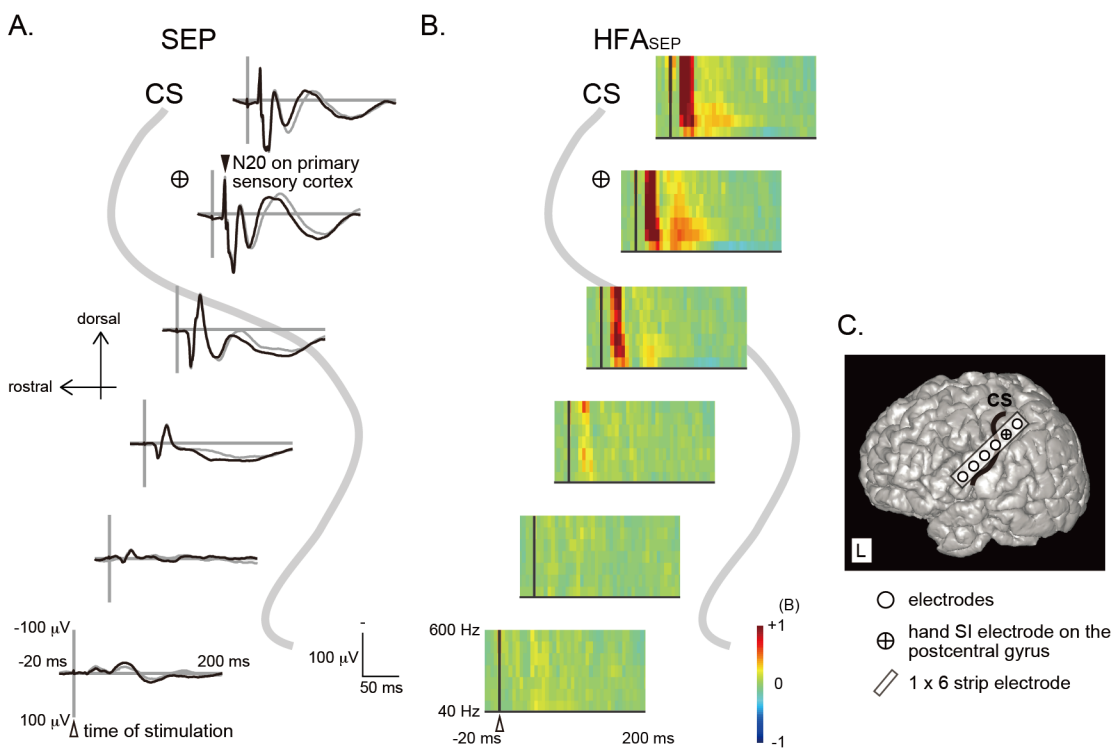
Fig 1. SEPs and HFAs$_{SEP}$ recorded from the peri-rolandic area and 3D-MRI (patient 1, left hemisphere). A: SEPs to right median nerve stimulation are plotted with subaverages (black and grey waveforms) across the CS identified on 3D-MRI (in a representative case). The vertical line corresponds to the time of median nerve stimulation (a white arrowhead). N20 component showing the maximum amplitude is identified on the primary somatosensory cortex (SI) (a black arrowhead). B: Time-frequency representation of SEP to right median nerve stimulation (HFA$_{SEP}$) by using the short-time Fourier Transform is shown across the CS. The frequency range is from 40 to 600 Hz. The vertical line corresponds to the time of median nerve stimulation (a white arrowhead). The averaged logarithmic power spectrum in reference to the baseline is calculated. Increase of power is indicated in red and decrease in blue. C: On 3D-MRI, subdural electrodes are plotted as white circles. A hand SI electrode is plotted as a white circle with a cross. Only electrodes at and around the hand SI and stimulus electrodes are shown in the figure. Since most of the induced high frequency activities were within 200 ms from the stimulus onset, we displayed the STFT results across the whole time points and frequencies in 3 dimensions (time, frequency, and power value) in a time window of 220 ms (from 20 ms before to 200 ms after the stimulus onset). SEP, somatosensory evoked potential; HFA, high frequency activity; CS, central sulcus.

doi:10.1371/journal.pone.0130461.g001
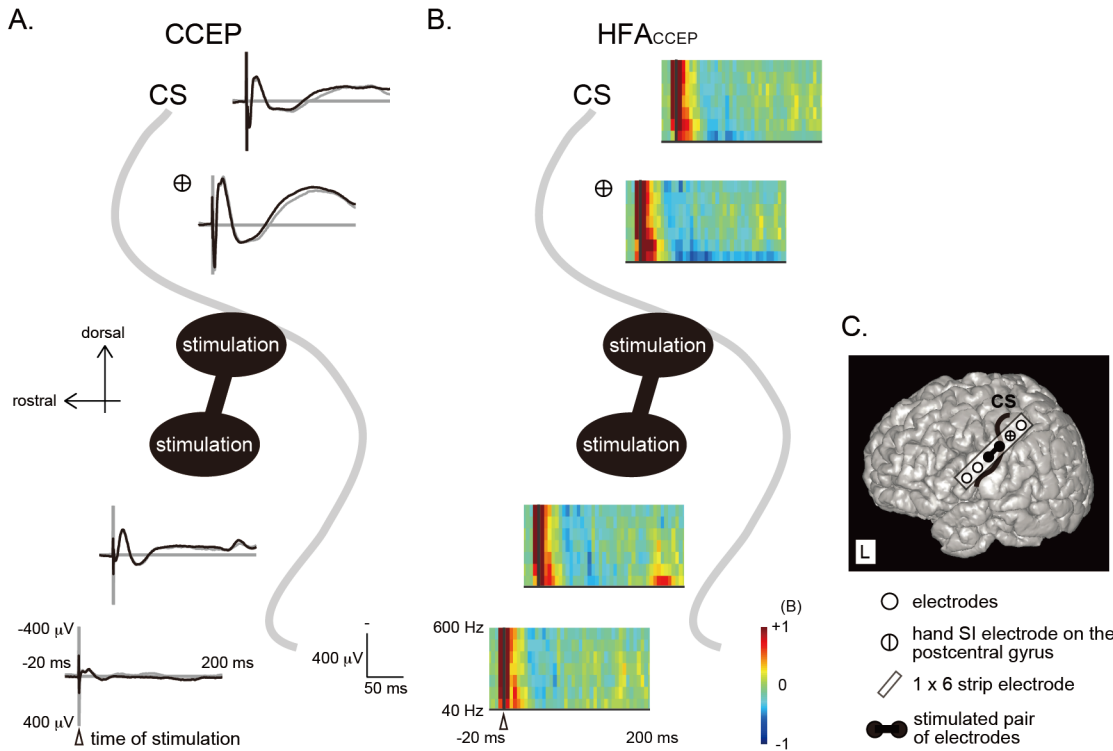
Fig 2. CCEPs and HFAs$_{CCEP}$ recorded from the peri-rolandic area and 3D-MRI (patient 1, left hemisphere). A: Single pulse stimulation was applied to the electrodes on the precentral gyrus and CCEPs were recorded time-locked to the stimuli (in a representative case). Two subaverages (black and grey waveforms) are shown. The vertical line corresponds to the time of single pulse stimulation (white arrowhead). B: Time-frequency representation of CCEP (HFA$_{CCEP}$) by using the short-time Fourier Transform. C: Electrodes on 3D-MRI. CCEP = cortico-cortical evoked potential. Other conventions are the same as for Fig 1.

doi:10.1371/journal.pone.0130461.g002

Statistical Analysis

The statistical analyses were performed by using the logarithmic power values of each SEP and CCEP responses (7 responses for HFA$_{SEP(N20)}$ and HFA$_{SEP(N80)}$, and 16 responses for HFA$_{CCEP(N1)}$ and HFA$_{CCEP(N2)}$). In this study we aimed to investigate whether there are differences of the distributions of logarithmic power spectra between the 4 groups. Repeated measures analysis of variance (RM-ANOVA) was adopted for the statistical investigation of the interactions with the power values in each frequency band as a within-group factor and with the aforementioned 4 groups [HFA$_{SEP(N20)}$, HFA$_{SEP(N80)}$, HFA$_{CCEP(N1)}$, and HFA$_{CCEP(N2)}$] as a between-group factor. As a post hoc analysis, we focused on the 4 comparisons between the groups: HFA$_{SEP(N20)}$ and HFA$_{CCEP(N1)}$, HFA$_{SEP(N80)}$ and HFA$_{CCEP(N2)}$, HFA$_{SEP(N20)}$ and HFA$_{SEP(N80)}$, and HFA$_{CCEP(N1)}$ and HFA$_{CCEP(N2)}$.

Results

Distribution of evoked responses and HFAs

Stimulation of the median nerve contralateral to the recording hemisphere elicited SEPs on the electrodes around the central sulcus (CS). As shown in the 3D-MRI of the representative case (patient 1L, Fig 1A), all the hand SI electrodes with the largest N20 were located on the post-central gyrus. As for the power spectra, HFAs$_{SEP}$ were recognized at and around the hand SI electrode (Fig 1B). The distribution of SEPs (N20 and N80) well corresponded to that of HFAs$_{SEP}$ (Fig 1C) in all patients. Regarding distribution of CCEPs and HFAs$_{CCEP}$, robust CCEP
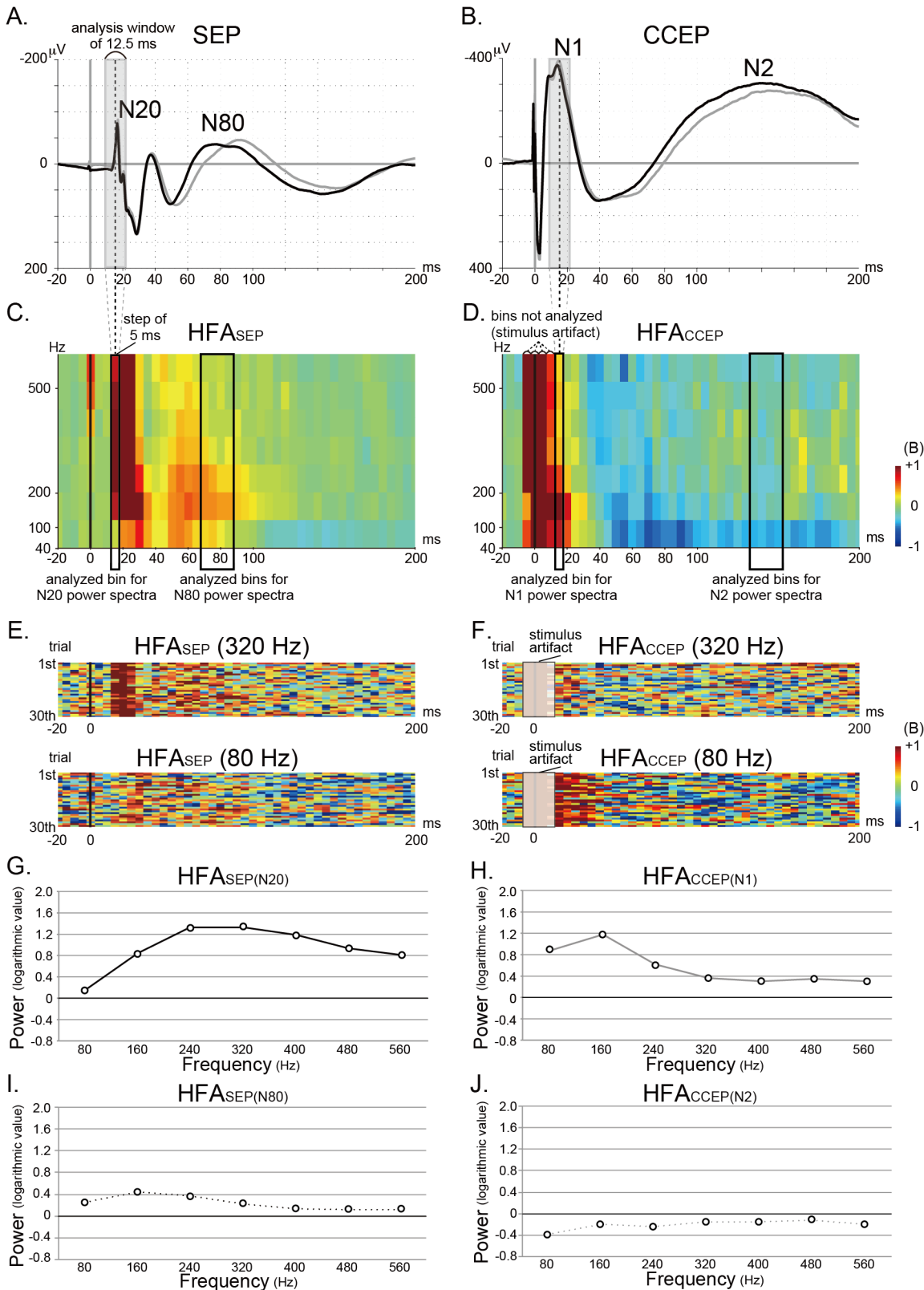
Fig 3. SEP, CCEP, HFA_SEP, and HFA_CCEP at SI (patient 1, left hemisphere). A-D: SEP (A), CCEP (B), HFA_SEP (C), and HFA_CCEP (D) recorded from the same hand SI electrode are shown in a representative case. The STFT was performed by using the short analysis-window of 25 points (12.5 ms) in order to differentiate the stimulus artifact from the CCEP N1 potential. Since the sliding window is set at 5 ms, each time bin (5ms-width) displays the STFT results of

the 12.5 ms analysis-window. For example, the 5 ms-time bin centered at 15 ms (highlighted by a black rectangle in C and D) corresponds to the results of 12.5 ms analysis-window (from 9 ms to 21.5 ms, centered at 15 ms; see shaded gray rectangle in A and B). The stimulus artifacts in CCEP last up to 3–4 ms from the stimulus onset. Therefore, the bins centered at -5, 0, 5, and 10 ms potentially include the stimulus artifacts and they are not analyzed. Because we put the transistor-transistor logic (TTL) pulse from the electric stimulator into the DC input of the EEG machine, and offline triggered the stimulus onset using a certain threshold with a Matlab-script, the trigger timing could have jitter within the sampling point, namely, 0.5 ms. This jitter is reflected in the representative CCEP waveform (B). As for the induced activities, the 5 ms time bins centered at -5 and 0 ms, which correspond to the results of 12.5 ms window centered at -5 and 0 ms, could include the stimulus artifact (D). E, F: The row traces (30 trials) of HFA_{SEP} (E) and HFA_{CCEP} (F) for the frequency bands centered at 80 and 320 Hz are shown. G-J: The power changes of $HFA_{SEP(N20)}$, $HFA_{CCEP(N1)}$, $HFA_{SEP(N80)}$, and $HFA_{CCEP(N2)}$ in reference to the baseline activity for each frequency band (every 80 Hz, centered at 80, 160, 240, 320, 400, 480, and 560 Hz) are plotted (G, H, I, and J).

responses (N1 and N2) and induced $HFAs_{CCEP}$ were recorded at the hand SI electrode by stimulating 16 stimulus sites (1–3 stimulus sites per patient: 1 site in patient 3, 2 sites in patient 1 (L), 1(R), and 6, and 3 sites in patient 2, 4, and 5) (see patient 1L, Fig 2A and 2B for example).

Comparison between HFA_{SEP} and HFA_{CCEP}

Fig 3 shows an example of comparison between SEP/HFA_{SEP} and CCEP/HFA_{CCEP} at the hand SI electrode. HFA_{SEP} and HFA_{CCEP} were shown with the three dimensional scales along the time window of 220 ms (Fig 3C and 3D). The row traces of HFA_{SEP} and HFA_{CCEP} for the frequency bands centered at 80 and 320 Hz, at which the HFA_{SEP} and HFA_{CCEP} presented the different power trend, are shown (Fig 3E and 3F). The power changes at the N20/N1 and N80/N2 peaks were then plotted in the two dimensional scale to show the distribution of the power change across the frequency bands (Fig 3G, 3H, 3I and 3J). The frequency band showing the maximal power change differed between $HFA_{SEP(N20)}$ and $HFA_{CCEP(N1)}$, $HFA_{SEP(N20)}$ and $HFA_{SEP(N80)}$, $HFA_{CCEP(N1)}$ and $HFA_{CCEP(N2)}$, and $HFA_{SEP(N80)}$ and $HFA_{CCEP(N2)}$ in this representative case (patient 1L). In order to compare the distribution of the power change between HFA_{SEP} and HFA_{CCEP} across patients, the mean and standard error of the logarithmic power values of all the responses are plotted across the frequency band for $HFA_{SEP(N20)}$, $HFA_{SEP(N80)}$, $HFA_{CCEP(N1)}$, and $HFA_{CCEP(N2)}$ (Fig 4). It showed a tendency that over 200 Hz, the $HFA_{SEP(N20)}$ power increased while $HFA_{CCEP(N1)}$ power decreased. RM-ANOVA showed statistically significant interactions between the 4 groups ($F(3,6) = 14.468$, $p < 0.05$). A post-hoc analysis showed significant interactions between $HFA_{SEP(N20)}$ and $HFA_{CCEP(N1)}$ ($F(1,6) = 19.409$, $p < 0.05$), $HFA_{SEP(N20)}$ and $HFA_{SEP(N80)}$ ($F(1,6) = 9.280$, $p < 0.05$), $HFA_{CCEP(N1)}$ and $HFA_{CCEP(N2)}$ ($F(1,6) = 22.494$, $p < 0.05$), and $HFA_{SEP(N80)}$ and $HFA_{CCEP(N2)}$ ($F(1,6) = 4.097$, $p < 0.05$). In other words, the distributions of power values differed between the 2 early components (CCEP N1 vs. SEP N20), as well as the 2 late components (CCEP N2 vs. SEP N80), and also between the early and late components of SEPs or CCEPs (SEP N1 vs. N2, CCEP N1 vs. N2).

Discussion

By applying SPES both to the peripheral nerve and directly to the cortex, we compared the HFAs overriding SEPs and CCEPs in the SI cortex. Stimulus-triggered HFAs behaved differently in terms of power distribution. As for the early components, $HFA_{SEP(N20)}$ power increased more in the frequency band above 200 Hz while $HFA_{CCEP(N1)}$ in the band below 200 Hz. As for the late components, statistically significant difference was also observed for the distributions of power spectra between $HFA_{SEP(N80)}$ and $HFA_{CCEP(N2)}$. Both HFA_{SEP} and HFA_{CCEP} showed different power distributions between early and late components. The present findings indicated that the human sensory cortex could produce different HFA profiles upon the different modes of input.
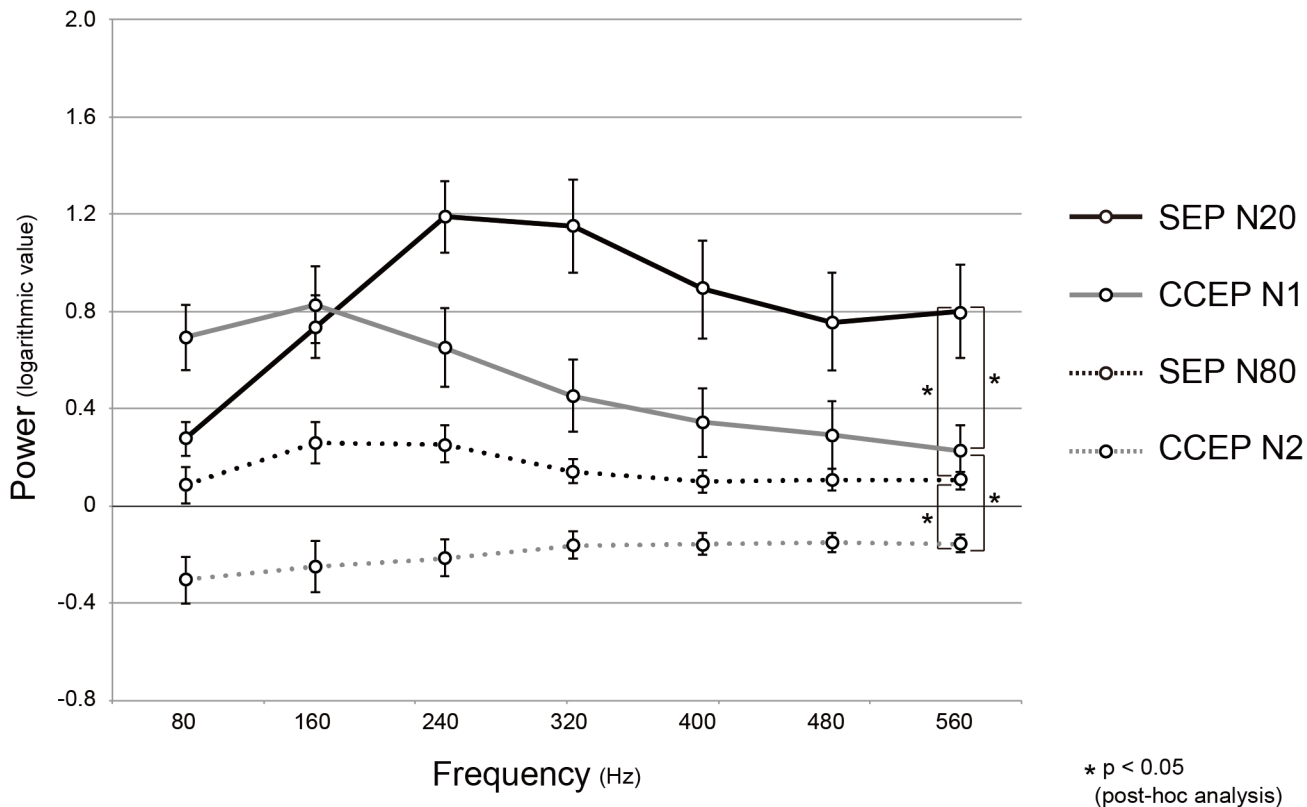
Fig 4. The distributions of logarithmic power values in reference to the baseline in each frequency band. As for the 4 groups, HFA$_{SEP(N20)}$ (a black solid line), HFA$_{CCEP(N1)}$ (a grey solid line), HFA$_{SEP(N80)}$ (a black dashed line) and HFA$_{CCEP(N2)}$ (a grey dashed line), all the power values of 7 hemispheres are averaged (mean ± SE). RM-ANOVA showed statistically significant interactions between the 4 groups. An asterisk indicates significant interaction between the 2 groups in the post-hoc analysis. Other conventions are the same as for Fig 3.

Stimulus induced early HFAs

As for the gamma activities recorded with macroelectrodes, Ray et al., by using a macaque monkey model, showed that the high gamma activity sensitively increased both in association with neuronal synchrony and firing rate [16]. In this regard, we think the HFA or 'broadband' gamma profiles were determined by neuronal synchrony and firing rate induced by the 2 modes of input in the present study. The HFAs were overriding or associated with either SEPs or CCEPs. SEPs are evoked through vertical, ascending projection fibers from the thalamus to the SI cortex, and CCEPs are evoked through horizontal association or commissural fibers based on the previous reports [51,60]. It is, therefore, plausible to ascribe the different gamma profiles between the early HFA components, HFA$_{SEP(N20)}$ and HFA$_{CCEP(N1)}$, to the different modes of impulse transmission through vertical projection vs. horizontal association/commissural fibers. The difference, then, could be explained by the different layer input from these 2 afferent fibers. Association and commissural fibers originate from the layer II and III and terminate mainly in the same layers elsewhere in the neocortex [61], while projection fibers from the thalamic relay (specific) nuclei, e.g. ventral posterolateral (VPL) in case of median nerve stimulation, terminate mainly in a rich arborization within the layer IV [62]. In this sense, it is indicated that different input modes played an important role in subsequent neuronal processing in terms of frequency tuning: neuronal synchrony in the high gamma range in case of horizontal transmission (HFA$_{CCEP(N1)}$ <200 Hz) vs. above the high gamma range in case of vertical transmission (HFA$_{SEP(N20)}$ >200 Hz). Several animal studies have indeed revealed that

frequency tuning (alpha, beta and gamma) for neural information processing differs according to the cortical layers, while that of faster activities above the conventional gamma range has not been well elucidated [45,63–68]. Since SI has the most developed layer IV in the neocortex, the inputs to the layer IV from the specific nuclei of the thalamus might give rise to neuronal synchrony in the higher frequency range than those to the layer II/III. A possible key player of the synchronization above 200 Hz is at least the fast-spiking interneuron which could produce the high frequency activities ranging 300–500 Hz [69–70]. In summary, different frequency profiles between $HFA_{SEP(N20)}$ and $HFA_{CCEP(N1)}$ is most likely due to the different propagation modes (vertical vs. horizontal), namely, the different terminal layers (layer IV vs. II/III) where afferent inputs arrive within SI. The layer IV contains the fast-spiking interneurons more than the layer II/III in SI. We speculate that the difference of the distribution of the fast-spiking interneurons may partly determine the most prominent frequency band of somatosensory and cortico-cortical HFAs in SI.

Another possible explanation is the influence of temporal jitters. 'Direct cortical response (DCR)' in the vicinity of the site of direct cortical stimulation has been extensively studied in various species [71–73]. Simultaneous surface and intracellular recording in animals revealed that the first negative components of DCR reflect oligosynaptic events in the local cortical circuits [46,74–75]. This local jitter of synaptic activity at the site of stimulation and at the target cortex in CCEPs might create the lesser synchronization as compared with the relatively synchronized disynaptic activities observed in SEPs.

The $HFA_{CCEP(N1)}$ has a frequency profile similar to HFA induced during various cognitive tasks ('cognitive HFA'). Cognitive HFAs have been reported to show a broadband shape in the power spectrum, which is probably organized by multiunit activities and/or local field potentials [16–17] or summation of membrane potential oscillations with different center frequencies [76]. Taking account of the similar frequency profile, cortico-cortical connections is highly likely to represent common mode of neuronal transmissions for various brain functions although the interaction to the 'centrencephalic' area would also influence the brain functions.

Stimulus induced late HFAs

The frequency profile was also different between the late components, $HFA_{SEP(N80)}$ and $HFA_{CCEP(N2)}$. Both SEP N80 and CCEP N2 have been considered to be late cortical components, although it is still not clear what they exactly reflect. One possible explanation for different frequency profiles in late HFAs is that the different stimulus types, a physiological stimulus through the peripheral nerve stimulation and a non-physiological stimulus directly applied to the cortex, could produce different intracortical neural processing in SI. In contrast to $HFA_{SEP(N80)}$ that had increased power in reference to the baseline activity, $HFA_{CCEP(N2)}$ showed a decline of the power value. This tendency is similar to the postspike depression seen in the spikes abnormally or non-physiologically produced by the epileptic focus [77–79]. It has been considered that this postspike depression reflects the decreased cortical excitability after paroxysmal depolarization shifts for epileptic spikes. In addition, by using an SPES technique similar to our CCEP method and recording multiunit activities, Alarcon et al. (2012) revealed that neural responses induced by SPES consist of brief synchronized burst firing and subsequent long suppression [80]. Therefore CCEP N2 could reflect an inhibitory process after the excitation reflected in N1 and $HFA_{CCEP(N1)}$. This might be an essential compensatory function of the human cerebral cortex. On the other hand, Matsuzaki et al. (2013), in their SPES/CCEP study in children, recently reported the increased gamma activities at the time of the end of N2 response in the visual cortex [81]. The difference between our study (decreased power) and theirs (increased power) could be explained by the difference of the cytoarchitecture, the

patients' age and the maturity of brain, or the phase of CCEP N2 response (peak vs. descending slope) when HFAs were observed. In our study, the bins centered at 80 Hz showed a tendency of the relative power decrease compared with the bins centered at 160 Hz, especially HFAs for CCEP. This is explained by the possibility that the frequency range centered at 80 Hz is mostly controlled by the inhibitory interneurons.

Clinical implications and limitations

Since this study was performed in patients with epilepsy or brain tumor, we should discuss whether we recorded pathological or physiological HFAs. In all patients, no epileptic HFAs or epileptic spikes were observed at the hand SI electrode. Together with the normal SEP configuration at and around the SI electrode, we considered the HFA_{SEP} and HFA_{CCEP} observed in the hand SI as physiological.

Pathological HFAs in the frequency range of ripple (100–200 Hz) and fast ripple (250- Hz) have recently attached considerable attention as a possible surrogate marker of epileptogenicity. By measuring the amplitude, CCEPs have been used for evaluating epileptogenicity or cortical excitability at and around the focus [55–56,82]. In this study we demonstrated the power increase ($HFA_{CCEP(N1)}$) and decrease ($HFA_{CCEP(N2)}$) were associated with CCEPs in the normally functioning SI. Besides the amplitude, the HFA correlates of CCEPs, namely $HFA_{CCEP(N1)}$ and $HFA_{CCEP(N2)}$, could also be clinically useful to evaluate the degree of abnormally enhanced cortical excitability and also surround inhibition at and around the epileptic focus, respectively.

There are several limitations in this study. First, the STFT analysis period was set after 15 ms in order to avoid the possible involvement of stimulus artifacts in the analysis. Therefore, some $HFAs_{CCEP}$ at the time range of 0 to 10 ms, such as HFA_{CCEP} overriding CCEP first volley or P1, which is the very first response reported in CCEP studies [60,83], could not be evaluated in this study. The relatively short analysis window (12.5 ms) and resultant broad frequency bin (80 Hz) did not allow us to analyze lower frequencies such as the beta or low gamma (below 40 Hz) band in the present study. Viswanathan et al. (2007) and Ray et al. (2008) reported that high-gamma (60–90 or 60–200 Hz) power could be a neural correlate of synchronized output of the cortex, while low-gamma (25–60 or 40–80 Hz) power could be a correlate of synchronized input to the cortex [16,84]. In this study, we mainly dealt with the activities of high-gamma range that reflects spike synchronization due to the 80 Hz frequency resolution. Therefore, our study suggests that the different propagation modes caused the frequency difference ($HFAs_{SEP}$ vs. $HFAs_{CCEP}$) within high-gamma range. Although the difference of low-gamma activities might have some influence on our results, synchronized input to the cortex would affect the neural correlate of synchronized output of the cortex. Second, it has been reported that human somatosensory evoked HFAs consist of 2 phases: early HFAs seen before the N20 peak and late HFAs after the peak. Possible generators of early HFAs are action potentials of the thalamocortical fibers at the time when they arrive at the area 3b (and area 1), and those of late HFAs are cortical fast inhibitory postsynaptic potentials or fast spiking interneurons in SI. In this study, we could not differentiate early and late HFAs due to the analysis window. Therefore, the difference of HFAs overriding SEP and CCEP might also reflect that of the presynaptic HFAs. Even in this case, the difference of the propagation modes and terminal layers between SEPs and CCEPs would be a key factor. Third, antiepileptic drugs might influence the occurrence of HFAs. The occurrence of pathological HFAs was reported to increase after reduction of antiepileptic drugs and decrease after induction of propofol [38,85]. Somatosensory evoked HFAs were reported to decrease both in frequency and amplitude during propofol administration [86–87]. In our study, although the SEP and CCEP recordings were not

performed on the same day in each patient, the amount of antiepileptic medication was almost the same between the 2 recordings. We, therefore, think that antiepileptic drugs hardly influenced the comparison between HFA$_{SEP}$ and HFA$_{CCEP}$. Fourth, we investigated the SI cortex since we could record and compare stimulus induced HFAs in response to both physiological (median nerve stimulation) vertical and non-physiological (direct electrical cortical stimulation) horizontal inputs. It is technically difficult to perform a similar study in the association cortex, but we assume the findings in SI could be applicable to the neocortex in general. Lastly, the sampling rate (2,000 Hz) and filter setting (0.016–600 Hz) prevented us to evaluate the HFA over 600 Hz. Our objective was to compare behaviors of the HFA involved in physiological and epileptic broadband gamma range, and we successfully demonstrated different behaviors in this frequency range for HFAs$_{CCEP}$ and HFAs$_{SEP}$. Future studies sacrificing the number of electrodes to increase the sampling rate would warrant investigation of higher HFA which was out of scope in the present study.

Supporting Information

S1 Text. Additional Data for Time Frequency Analysis.
(DOC)

S1 Fig. CCEPs and HFAs$_{CCEP}$ in an additional study to validate the influence of the stimulus artifacts. A: A configuration of grid electrodes placed on each hemisphere of a dead brain of a pig. Shaded circles indicate 2 stimulated pairs of electrodes. B: CCEPs recorded time-locked to the single pulse stimulation applied to the electrodes labeled as "1" in S1A Fig. Two subaverages (black and grey waveforms) are shown. We displayed in a time window of 220 ms (from 20 ms before to 200 ms after the stimulus onset) in the same way as the original Figs 1–3. The vertical line corresponds to the time of single pulse stimulation (white arrowhead). C: A CCEP response recorded from the electrode adjacent to the stimulus sites (dotted square). D: Time-frequency representation of CCEP (HFA$_{CCEP}$) by using the short-time Fourier Transform. The frequency range is from 40 to 600 Hz. The vertical line corresponds to the time of single pulse stimulation (a white arrowhead). The averaged logarithmic power spectrum in reference to the baseline is calculated. Increase of power is indicated in red and decrease in blue. E: An HFA$_{CCEP}$ recorded from the same electrode as S1C Fig. In this particular example, the stimulus artifact, indicated in dark red suggestive of extraordinary power increase, affected the time bin centered at 5 ms and did not affect the bins centered at 10 ms and 15 ms. In case of stimulation of another pair of electrodes (labeled as "2" in S1A Fig), the stimulus artifact never influenced to the bin centered at 15 ms.
(TIF)

Author Contributions

Conceived and designed the experiments: KK RM MM AI. Performed the experiments: KK RM KU AS. Analyzed the data: KK RM. Contributed reagents/materials/analysis tools: T. Kunieda T. Kikuchi NM SM HF. Wrote the paper: KK RM MM AI. Coordinated and directed the project: RM RT AI.

References

1. Crone NE, Miglioretti DL, Gordon B, Lesser RP. Functional mapping of human sensorimotor cortex with electrocorticographic spectral analysis. II. Event-related synchronization in the gamma band. Brain. 1998; 121: 2301–2315. PMID: 9874481

2. Bragin A, Engel J Jr., Wilson CL, Fried I, Buzsaki G. High-frequency oscillations in human brain. Hippocampus. 1999; 9: 137–142. PMID: 10226774

3. Bragin A, Engel J Jr., Wilson CL, Fried I, Mathern GW. Hippocampal and entorhinal cortex high-frequency oscillations (100–500 Hz) in human epileptic brain and in kainic acid-treated rats with chronic seizures. Epilepsia. 1999; 40: 127–137. PMID: 9952257

4. Ohara S, Ikeda A, Kunieda T, Yazawa S, Baba K, Nagamine T, et al. Movement-related change of electrocorticographic activity in human supplementary motor area proper. Brain. 2000; 123: 1203–1215. PMID: 10825358

5. Miller KJ, Leuthardt EC, Schalk G, Rao RP, Anderson NR, Moran DW, et al. Spectral changes in cortical surface potentials during motor movement. J Neurosci. 2007; 27: 2424–2432. PMID: 17329441

6. Miller KJ, Zanos S, Fetz EE, den Nijs M, Ojemann JG. Decoupling the cortical power spectrum reveals real-time representation of individual finger movements in humans. J Neurosci. 2009; 29: 3132–3137. doi: 10.1523/JNEUROSCI.5506-08.2009 PMID: 19279250

7. Sinai A, Bowers CW, Crainiceanu CM, Boatman D, Gordon B, Lesser RP, et al. Electrocorticographic high gamma activity versus electrical cortical stimulation mapping of naming. Brain. 2005; 128: 1556–1570. PMID: 15817517

8. Tanji K, Suzuki K, Delorme A, Shamoto H, Nakasato N. High-frequency gamma-band activity in the basal temporal cortex during picture-naming and lexical-decision tasks. J Neurosci. 2005; 25: 3287–3293. PMID: 15800183

9. Ray S, Niebur E, Hsiao SS, Sinai A, Crone NE. High-frequency gamma activity (80–150Hz) is increased in human cortex during selective attention. Clin Neurophysiol. 2008; 119: 116–133. PMID: 18037343

10. Edwards E, Soltani M, Deouell LY, Berger MS, Knight RT. High gamma activity in response to deviant auditory stimuli recorded directly from human cortex. J Neurophysiol. 2005; 94: 4269–4280. PMID: 16093343

11. Sinai A, Crone NE, Wied HM, Franaszczuk PJ, Miglioretti D, Boatman-Reich D. Intracranial mapping of auditory perception: event-related responses and electrocortical stimulation. Clin Neurophysiol. 2009; 120: 140–149. doi: 10.1016/j.clinph.2008.10.152 PMID: 19070540

12. Tallon-Baudry C, Bertrand O, Henaff MA, Isnard J, Fischer C. Attention modulates gamma-band oscillations differently in the human lateral occipital cortex and fusiform gyrus. Cereb Cortex. 2005; 15: 654–662. PMID: 15371290

13. Brunel N, Wang XJ. What determines the frequency of fast network oscillations with irregular neural discharges? I. Synaptic dynamics and excitation-inhibition balance. J Neurophysiol. 2003; 90: 415–430. PMID: 12611969

14. Mann EO, Radcliffe CA, Paulsen O. Hippocampal gamma-frequency oscillations: from interneurones to pyramidal cells, and back. J Physiol. 2005; 562: 55–63. PMID: 15539391

15. Bartos M, Vida I, Jonas P. Synaptic mechanisms of synchronized gamma oscillations in inhibitory interneuron networks. Nat Rev Neurosci. 2007; 8: 45–56. PMID: 17180162

16. Ray S, Crone NE, Niebur E, Franaszczuk PJ, Hsiao SS. Neural correlates of high-gamma oscillations (60–200 Hz) in macaque local field potentials and their potential implications in electrocorticography. J Neurosci. 2008; 28: 11526–11536. doi: 10.1523/JNEUROSCI.2848-08.2008 PMID: 18987189

17. Miller KJ. Broadband spectral change: evidence for a macroscale correlate of population firing rate? J Neurosci. 2010; 30: 6477–6479. doi: 10.1523/JNEUROSCI.6401-09.2010 PMID: 20463210

18. Hermes D, Miller KJ, Wandell BA, Winawer J. Stimulus Dependence of Gamma Oscillations in Human Visual Cortex. Cereb Cortex. 2015; 36: 1–15.

19. Cracco RQ, Cracco JB. Somatosensory evoked potential in man: far field potentials. Electroencephalogr Clin Neurophysiol. 1976; 41: 460–466. PMID: 61849

20. Abbruzzese M, Favale E, Leandri M, Ratto S. New subcortical components of the cerebral somatosensory evoked potential in man. Acta Neurol Scand. 1978; 58: 325–332. PMID: 742350

21. Eisen A, Roberts K, Low M, Hoirch M, Lawrence P. Questions regarding the sequential neural generator theory of the somatosensory evoked potential raised by digital filtering. Electroencephalogr Clin Neurophysiol. 1984; 59: 388–395. PMID: 6205866

22. Emerson RG, Sgro JA, Pedley TA, Hauser WA. State-dependent changes in the N20 component of the median nerve somatosensory evoked potential. Neurology. 1988; 38: 64–68. PMID: 3336466

23. Yamada T, Kameyama S, Fuchigami Y, Nakazumi Y, Dickins QS, Kimura J. Changes of short latency somatosensory evoked potential in sleep. Electroencephalogr Clin Neurophysiol. 1988; 70: 126–136. PMID: 2456191

24. Emori T, Yamada T, Seki Y, Yasuhara A, Ando K, Honda Y, et al. Recovery functions of fast frequency potentials in the initial negative wave of median SEP. Electroencephalogr Clin Neurophysiol. 1991; 78: 116–123. PMID: 1704834

25. Curio G, Mackert BM, Burghoff M, Koetitz R, Abraham-Fuchs K, Harer W. Localization of evoked neuro-magnetic 600 Hz activity in the cerebral somatosensory system. Electroencephalogr Clin Neurophysiol. 1994; 91: 483–487. PMID: 7529687

26. Hashimoto I, Mashiko T, Imada T. Somatic evoked high-frequency magnetic oscillations reflect activity of inhibitory interneurons in the human somatosensory cortex. Electroencephalogr Clin Neurophysiol. 1996; 100: 189–203. PMID: 8681860

27. Sonoo M, Genba-Shimizu K, Mannen T, Shimizu T. Detailed analysis of the latencies of median nerve somatosensory evoked potential components, 2: Analysis of subcomponents of the P13/14 and N20 potentials. Electroencephalogr Clin Neurophysiol. 1997; 104: 296–311. PMID: 9246067

28. Ozaki I, Suzuki C, Yaegashi Y, Baba M, Matsunaga M, Hashimoto I. High frequency oscillations in early cortical somatosensory evoked potentials. Electroencephalogr Clin Neurophysiol. 1998; 108: 536–542. PMID: 9872424

29. Curio G. Linking 600-Hz "spikelike" EEG/MEG wavelets ("sigma-bursts") to cellular substrates: concepts and caveats. J Clin Neurophysiol. 2000; 17: 377–396. PMID: 11012041

30. Ikeda H, Leyba L, Bartolo A, Wang Y, Okada YC. Synchronized spikes of thalamocortical axonal terminals and cortical neurons are detectable outside the pig brain with MEG. J Neurophysiol. 2002; 87: 626–630. PMID: 11784777

31. Curio G, Mackert BM, Burghoff M, Neumann J, Nolte G, Scherg M, et al. Somatotopic source arrangement of 600 Hz oscillatory magnetic fields at the human primary somatosensory hand cortex. Neurosci Lett. 1997; 234: 131–134. PMID: 9364515

32. Gobbele R, Waberski TD, Simon H, Peters E, Klostermann F, Curio G, et al. Different origins of low- and high-frequency components (600 Hz) of human somatosensory evoked potentials. Clin Neurophysiol. 2004; 115: 927–937. PMID: 15003775

33. Gobbele R, Waberski TD, Dieckhofer A, Kawohl W, Klostermann F, Curio G, et al. Patterns of disturbed impulse propagation in multiple sclerosis identified by low and high frequency somatosensory evoked potential components. J Clin Neurophysiol. 2003; 20: 283–290. PMID: 14530742

34. Coppola G, Vandenheede M, Di Clemente L, Ambrosini A, Fumal A, De Pasqua V, et al. Somatosensory evoked high-frequency oscillations reflecting thalamo-cortical activity are decreased in migraine patients between attacks. Brain. 2005; 128: 98–103. PMID: 15563513

35. Restuccia D, Valeriani M, Della Marca G. Giant subcortical high-frequency SEPs in idiopathic generalized epilepsy: a protective mechanism against seizures? Clin Neurophysiol. 2007; 118: 60–68. PMID: 17097917

36. Ozaki I, Hashimoto I. Exploring the physiology and function of high-frequency oscillations (HFOs) from the somatosensory cortex. Clin Neurophysiol. 2011; 122: 1908–1923. doi: 10.1016/j.clinph.2011.05.023 PMID: 21724458

37. Urrestarazu E, Chander R, Dubeau F, Gotman J. Interictal high-frequency oscillations (100–500 Hz) in the intracerebral EEG of epileptic patients. Brain. 2007; 130: 2354–2366. PMID: 17626037

38. Zijlmans M, Jacobs J, Zelmann R, Dubeau F, Gotman J. High-frequency oscillations mirror disease activity in patients with epilepsy. Neurology. 2009; 72: 979–986. doi: 10.1212/01.wnl.0000344402.20334.81 PMID: 19289737

39. Jacobs J, Zijlmans M, Zelmann R, Chatillon CE, Hall J, Olivier A, et al. High-frequency electroencephalographic oscillations correlate with outcome of epilepsy surgery. Ann Neurol. 2010; 67: 209–220. doi: 10.1002/ana.21847 PMID: 20225281

40. Bragin A, Wilson CL, Engel J Jr. Voltage depth profiles of high-frequency oscillations after kainic acid-induced status epilepticus. Epilepsia 48 Suppl. 2007; 5: 35–40.

41. Bragin A, Benassi SK, Kheiri F, Engel J Jr. Further evidence that pathologic high-frequency oscillations are bursts of population spikes derived from recordings of identified cells in dentate gyrus. Epilepsia. 2011; 52: 45–52. doi: 10.1111/j.1528-1167.2011.03235.x PMID: 21967361

42. Ketchum KL, Haberly LB. Synaptic events that generate fast oscillations in piriform cortex. J Neurosci. 1993; 13: 3980–3985. PMID: 8366356

43. Rolston JD, Laxpati NG, Gutekunst CA, Potter SM, Gross RE. Spontaneous and evoked high-frequency oscillations in the tetanus toxin model of epilepsy. Epilepsia. 2010; 51: 2289–2296. doi: 10.1111/j.1528-1167.2010.02753.x PMID: 20946126

44. Le Van Quyen M, Bragin A, Staba R, Crepon B, Wilson CL, Engel J Jr. Cell type-specific firing during ripple oscillations in the hippocampal formation of humans. J Neurosci. 2008; 28: 6104–6110. doi: 10.1523/JNEUROSCI.0437-08.2008 PMID: 18550752

45. Wang XJ. Neurophysiological and computational principles of cortical rhythms in cognition. Physiol Rev. 2010; 90: 1195–1268. doi: 10.1152/physrev.00035.2008 PMID: 20664082

46. Matsumoto R, Nair DR, LaPresto E, Najm I, Bingaman W, Shibasaki H, et al. Functional connectivity in the human language system: a cortico-cortical evoked potential study. Brain. 2004; 127: 2316–2330. PMID: 15269116

47. Greenlee JD, Oya H, Kawasaki H, Volkov IO, Severson MA 3rd, Howard MA 3rd, et al. Functional connections within the human inferior frontal gyrus. J Comp Neurol. 2007; 503: 550–559. PMID: 17534935

48. Lacruz ME, Garcia Seoane JJ, Valentin A, Selway R, Alarcon G. Frontal and temporal functional connections of the living human brain. Eur J Neurosci. 2007; 26: 1357–1370. PMID: 17767512

49. Matsumoto R, Nair DR, LaPresto E, Bingaman W, Shibasaki H, Luders HO. Functional connectivity in human cortical motor system: a cortico-cortical evoked potential study. Brain. 2007; 130: 181–197. PMID: 17046857

50. Matsumoto R, Imamura H, Inouchi M, Nakagawa T, Yokoyama Y, Matsuhashi M, et al. Left anterior temporal cortex actively engages in speech perception: A direct cortical stimulation study. Neuropsychologia. 2011; 49: 1350–1354. doi: 10.1016/j.neuropsychologia.2011.01.023 PMID: 21251921

51. Matsumoto R, Nair DR, Ikeda A, Fumuro T, Lapresto E, Mikuni N, et al. Parieto-frontal network in humans studied by cortico-cortical evoked potential. Hum Brain Mapp. 2012; 33: 2856–2872. doi: 10.1002/hbm.21407 PMID: 21928311

52. Swann NC, Cai W, Conner CR, Pieters TA, Claffey MP, George JS, et al. Roles for the pre-supplementary motor area and the right inferior frontal gyrus in stopping action: electrophysiological responses and functional and structural connectivity. Neuroimage. 2012; 59: 2860–2870. doi: 10.1016/j.neuroimage.2011.09.049 PMID: 21979383

53. Terada K, Umeoka S, Usui N, Baba K, Usui K, Fujitani S, et al. Uneven interhemispheric connections between left and right primary sensori-motor areas. Hum Brain Mapp. 2012; 33: 14–26. doi: 10.1002/hbm.21189 PMID: 21337473

54. Entz L, Toth E, Keller CJ, Bickel S, Groppe DM, Fabo D, et al. Evoked effective connectivity of the human neocortex. Hum Brain Mapp. 2014; 35: 5736–5753. doi: 10.1002/hbm.22581 PMID: 25044884

55. Iwasaki M, Enatsu R, Matsumoto R, Novak E, Thankappen B, Piao Z, et al. Accentuated cortico-cortical evoked potentials in neocortical epilepsy in areas of ictal onset. Epileptic Disord. 2010; 12: 292–302. doi: 10.1684/epd.2010.0334 PMID: 20952353

56. Enatsu R, Piao Z, O'Connor T, Horning K, Mosher J, Burgess R, et al. Cortical excitability varies upon ictal onset patterns in neocortical epilepsy: a cortico-cortical evoked potential study. Clin Neurophysiol. 2012; 123: 252–260. doi: 10.1016/j.clinph.2011.06.030 PMID: 21802356

57. Matsumoto R, Ikeda A, Ohara S, Matsuhashi M, Baba K, Yamane F, et al. Motor-related functional subdivisions of human lateral premotor cortex: epicortical recording in conditional visuomotor task. Clin Neurophysiol. 2003; 114: 1102–1115. PMID: 12804679

58. Matsumoto R, Nair D. Cortico-cortical evoked potentials to define eloquent cortex. In: Lüders HO, editor. Textbook of Epilepsy Surgery. London: Informa UK Ltd; 2008. pp 1049–1059.

59. Crone NE, Boatman D, Gordon B, Hao L. Induced electrocorticographic gamma activity during auditory perception. Brazier Award-winning article, 2001. Clin Neurophysiol. 2001; 112: 565–582. PMID: 11275528

60. Yamao Y, Matsumoto R, Kunieda T, Arakawa Y, Kobayashi K, Usami K, et al. Intraoperative dorsal language network mapping by using single-pulse electrical stimulation. Hum Brain Mapp. 2014; 35: 4345–4361. doi: 10.1002/hbm.22479 PMID: 24615889

61. Lorente de No R. Cerebral cortex: architecture, intracortical connections, motor projections. In: Fulton JF, editor. Physiology of the nervous system, 3rd edn. Oxford: Oxford University Press; 1949. pp 288–330.

62. Arnold PB, Li CX, Waters RS. Thalamocortical arbors extend beyond single cortical barrels: an in vivo intracellular tracing study in rat. Exp Brain Res. 2001; 136: 152–168. PMID: 11206278

63. Gray CM, McCormick DA. Chattering cells: superficial pyramidal neurons contributing to the generation of synchronous oscillations in the visual cortex. Science. 1996; 274: 109–113. PMID: 8810245

64. Cunningham MO, Whittington MA, Bibbig A, Roopun A, LeBeau FE, Vogt A, et al. A role for fast rhythmic bursting neurons in cortical gamma oscillations in vitro. Proc Natl Acad Sci U S A. 2004; 101: 7152–7157. PMID: 15103017

65. Roopun AK, Middleton SJ, Cunningham MO, LeBeau FE, Bibbig A, Whittington MA, et al. A beta2-frequency (20–30 Hz) oscillation in nonsynaptic networks of somatosensory cortex. Proc Natl Acad Sci U S A. 2006; 103: 15646–15650. PMID: 17030821

66. Buffalo EA, Fries P, Landman R, Buschman TJ, Desimone R. Laminar differences in gamma and alpha coherence in the ventral stream. Proc Natl Acad Sci U S A. 2011; 108: 11262–11267. doi: 10.1073/pnas.1011284108 PMID: 21690410

67. Ray S, Maunsell JH. Different origins of gamma rhythm and high-gamma activity in macaque visual cortex. PLoS Biol. 2011; 9:e1000610. doi: 10.1371/journal.pbio.1000610 PMID: 21532743

68. Scheffer-Teixeira R, Belchior H, Leao RN, Ribeiro S, Tort AB. On high-frequency field oscillations (>100 Hz) and the spectral leakage of spiking activity. J Neurosci. 2013; 33: 1535–1539. doi: 10.1523/JNEUROSCI.4217-12.2013 PMID: 23345227

69. Connors BW, Gutnick MJ. Intrinsic firing patterns of diverse neocortical neurons. Trends Neurosci. 1990; 13: 99–104. PMID: 1691879

70. Jones MS, MacDonald KD, Choi B, Dudek FE, Barth DS. Intracellular correlates of fast (>200 Hz) electrical oscillations in rat somatosensory cortex. J Neurophysiol. 2000; 84: 1505–1518. PMID: 10980023

71. Adrian ED. The spread of activity in the cerebral cortex. J Physiol. 1936; 88: 127–161. PMID: 16994811

72. Purpura DP, Pool JL, Ransohoff J, Frumin MJ, Housepian EM. Observations on evoked dendritic potentials of human cortex. Electroencephalogr Clin Neurophysiol. 1957; 9: 453–459. PMID: 13447852

73. Goldring S, Harding GW, Gregorie EM. Distinctive electrophysiological characteristics of functionally discrete brain areas: a tenable approach to functional localization. J Neurosurg. 1994; 80: 701–709. PMID: 8151350

74. Li CL, Chou SN. Cortical intracellular synaptic potentials and direct cortical stimulation. J Cell Comp Physiol. 1962; 60: 1–16. PMID: 14464979

75. Sugaya E, Goldring S, O'Leary JL. Intracellular potentials associated with direct cortical response and seizure discharge in cat. Electroencephalogr Clin Neurophysiol. 1964; 17: 661–669. PMID: 14240859

76. Crone NE, Korzeniewska A, Franaszczuk PJ. Cortical gamma responses: searching high and low. Int J Psychophysiol. 2011; 79: 9–15. doi: 10.1016/j.ijpsycho.2010.10.013 PMID: 21081143

77. Ayala GF, Dichter M, Gumnit RJ, Matsumoto H, Spencer WA. Genesis of epileptic interictal spikes. New knowledge of cortical feedback systems suggests a neurophysiological explanation of brief paroxysms. Brain Res. 1973; 52: 1–17. PMID: 4573428

78. Neckelmann D, Amzica F, Steriade M. Changes in neuronal conductance during different components of cortically generated spike-wave seizures. Neuroscience. 2000; 96: 475–485. PMID: 10717428

79. Urrestarazu E, Jirsch JD, LeVan P, Hall J, Avoli M, Dubeau F, et al. High-frequency intracerebral EEG activity (100–500 Hz) following interictal spikes. Epilepsia. 2006; 47: 1465–1476. PMID: 16981862

80. Alarcon G, Martinez J, Kerai SV, Lacruz ME, Quiroga RQ, Selway RP, et al. In vivo neuronal firing patterns during human epileptiform discharges replicated by electrical stimulation. Clin Neurophysiol. 2012; 123: 1736–1744. doi: 10.1016/j.clinph.2012.02.062 PMID: 22410162

81. Matsuzaki N, Juhasz C, Asano E. Cortico-cortical evoked potentials and stimulation-elicited gamma activity preferentially propagate from lower- to higher-order visual areas. Clin Neurophysiol. 2013; 124: 1290–1296. doi: 10.1016/j.clinph.2013.02.007 PMID: 23523110

82. Matsumoto R, Kinoshita M, Taki J, Hitomi T, Mikuni N, Shibasaki H, et al. In vivo epileptogenicity of focal cortical dysplasia: a direct cortical paired stimulation study. Epilepsia. 2005; 46: 1744–1749. PMID: 16302853

83. Terada K, Usui N, Umeoka S, Baba K, Mihara T, Matsuda K, et al. Interhemispheric connection of motor areas in humans. J Clin Neurophysiol. 2008; 25: 351–356. doi: 10.1097/WNP.0b013e31818f4fec PMID: 18997625

84. Viswanathan A, Freeman RD. Neurometabolic coupling in cerebral cortex reflects synaptic more than spiking activity. Nat Neurosci. 2007; 10: 1308–1312. PMID: 17828254

85. Zijlmans M, Huiskamp GM, Cremer OL, Ferrier CH, van Huffelen AC, Leijten FS. Epileptic high-frequency oscillations in intraoperative electrocorticography: the effect of propofol. Epilepsia. 2012; 53: 1799–1809. doi: 10.1111/j.1528-1167.2012.03650.x PMID: 22984839

86. Klostermann F, Funk T, Vesper J, Siedenberg R, Curio G. Propofol narcosis dissociates human intrathalamic and cortical high-frequency (> 400 hz) SEP components. Neuroreport. 2000; 11: 2607–2610. PMID: 10943731

87. Urasaki E, Genmoto T, Yokota A, Maeda R, Akamatsu N. Effects of general anesthesia on high-frequency oscillations in somatosensory evoked potentials. J Clin Neurophysiol. 2006; 23: 426–430. PMID: 17016153